The over-all distribution is then one which is sharply peaked at $\theta=\theta_l$, and decreasing monotonically as θ increases away from θ_l.

On the basis of this argument we would therefore expect all direct surface reactions to have similar angular distributions, with the position of the main first peak being determined largely by the kinematics, plus the fact that the interaction occurs in the surface shell. Of course any type of particle may be considered the incident particle without change in the arguments.

The semiclassical arguments employed here are clearly not adequate for deriving all details of the angular distribution. From a quantum mechanical description one expects an oscillatory distribution (e.g., dotted curve of Fig. 7) with the semiclassical distribution providing an envelope for the peak maxima.

PHYSICAL REVIEW VOLUME 106, NUMBER 2 APRIL 15, 1957

Elastic Scattering of 40-Mev Protons by He^4†

MORTON K. BRUSSEL AND JOHN H. WILLIAMS
School of Physics, University of Minnesota, Minneapolis, Minnesota
(Received November 19, 1956)

Monoenergetic 39.8-Mev protons, accelerated by the Minnesota linear accelerator, were scattered by purified helium gas. The elastically scattered protons were detected at forty-three angles between 4° and 135° and the results are presented in terms of the absolute differential scattering cross section per unit solid angle in the center-of-mass system of coordinates. Definite minima and maxima in the variation of cross section with angle were observed.

INTRODUCTION

THE elastic scattering of protons by He^4 has been the subject of intensive experimental and theoretical studies over a wide range of incident proton energies at several laboratories. Early work by Freier, Lampi, Sleator, and Williams[1] with protons of energy up to 3.5 Mev was analyzed in terms of phase shifts by Critchfield and Dodder.[2] An ordering of the $P_{\frac{3}{2}}$, $P_{\frac{1}{2}}$ doublet of the compound nucleus states of Li^5 was made possible by the work of Heusinkveld and Freier[3] who examined the polarization of protons scattered by He^4. Later experimental work with 5.82-Mev protons by Kreger, Kerman, and Jentscke[4] and with 9.48-Mev protons by Putnam[5] has been analyzed by Dodder and Gammel.[6] Further observations by Freemantle *et al.*[7] at 9.55 Mev agreed qualitatively with Putnam's observations which were accurately confirmed by Williams and Rasmussen[8] at 9.76 Mev. At higher energies Brockman,[9] who also carried out a phase shift analysis, and Cork,[10] and Wickersham[11] obtained differential cross sections for the elastic scattering by He of 17.45-Mev, 31.6-Mev, and 27.9-Mev protons, respectively, over various angular ranges. At Harvard, Teem *et al.*[12] have made a more extensive set of such observations with 93-Mev protons which reveal for the first time definite minima and maxima in the variation of the differential cross section for (p,α) scattering with angle.

In view of the extensive experimental data and the theoretical interpretations of (p,α) scattering now available at energies less than 10 Mev, the paucity of information at higher energies and the degree of interest in the (p,α) process as a tool for measuring the state of polarization of high-energy proton beams, the present measurements were undertaken as part of a program to investigate proton scattering phenomena at 40 Mev with the University of Minnesota linear accelerator.

EXPERIMENTAL APPARATUS

Protons of 39.85 Mev are available from the second section of the Minnesota linear accelerator. The characteristics of this beam are as follows: estimated energy spread, less than ± 0.20 Mev; approximate diameter of beam, $\frac{1}{2}$ inch; angular divergence of beam, less than 1.5×10^{-3} radian; pulse length, more than 150 microseconds; instantaneous current, 9×10^{-6} ampere; time average current, 4×10^{-8} ampere. These protons, after being magnetically deflected away from the principal axis of the accelerator, traverse a strong-focusing quadrupole magnet and travel approximately thirty feet into a shielded experimental area.

A general purpose scattering apparatus, shown in Fig. 1, which was developed for the study of nuclear

† Work supported in part by the U. S. Atomic Energy Commission.

[1] Freier, Lampi, Sleator, and Williams, Phys. Rev. **75**, 1345 (1949).
[2] C. L. Critchfield and D. C. Dodder, Phys. Rev. **76**, 602 (1949).
[3] M. Heusinkveld and G. Freier, Phys. Rev. **85**, 80 (1952).
[4] Kreger, Kerman, and Jentscke, Phys. Rev. **86**, 593 (1952).
[5] T. M. Putnam, Phys. Rev. **87**, 932 (1952).
[6] D. C. Dodder and J. L. Gammel, Phys. Rev. **88**, 520 (1952).
[7] Freemantle, Grotdal, Gibson, McKeague, Prowse, and Rotblat, Phil. Mag. **45**, 1090 (1954).
[8] J. H. Williams and S. W. Rasmussen, Phys. Rev. **98**, 56 (1955).
[9] K. W. Brockman, Jr., Phys. Rev. **102**, 391 (1956).
[10] B. Cork, Phys. Rev. **89**, 78 (1953).
[11] A. F. Wickersham, University of California Radiation Laboratory Report UCRL-2662 (unpublished).
[12] J. Teem (private communication), and Teem, Selove, and Kruse, Phys. Rev. **98**, 259(A) (1955).

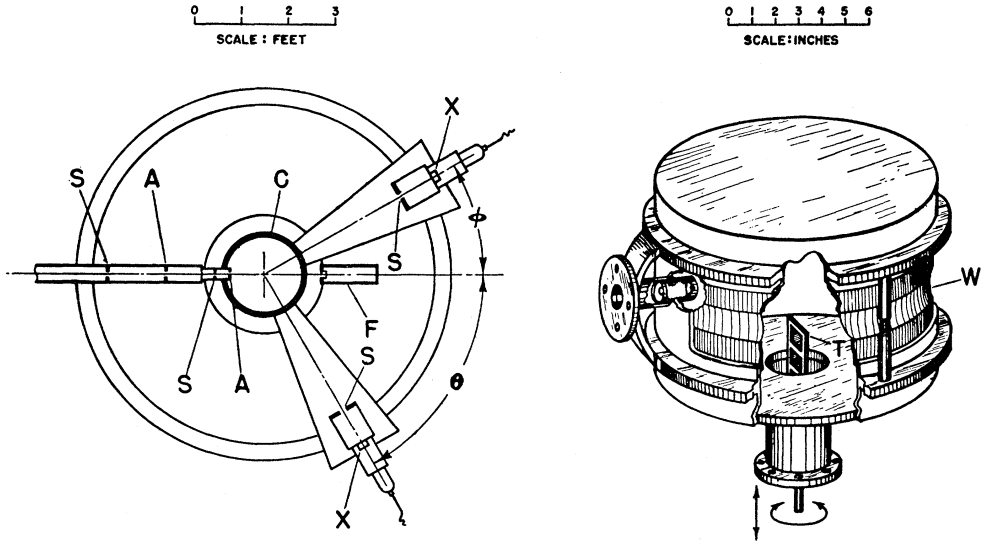

FIG. 1. Schematic drawing of eight-foot diameter scattering stand. Plan view shows the two tables which are independently rotatable about the central vertical axis, defining slits S, antiscattering slits A, crystal detectors X, Faraday cage F, and central vacuum chamber C. The perspective drawing is a more detailed view of C showing the Mylar window W and movable target holder T.

processes occurring in both solid and gaseous targets, was employed in this study. The proton beam enters from the left through collimating and antiscattering apertures and passes over the central vertical axis of the apparatus. The targets, in this case purified He gas at one atmosphere pressure, are contained in a central cylinder. The principal feature of the target chamber is a Mylar-covered exit window extending from 166° on one side of the beam axis to 170° on the other side. The unscattered beam emerges at zero degrees and after passing through a few inches of air enters a Faraday cage of conventional design which serves to measure the incident proton current. The scattered protons also leave the target chamber through the Mylar window, are then collimated by slits defining the angle of observation, and finally are detected by passing through an aperture of known area into a NaI(Tl) crystal. A similar monitor counter, mounted at a fixed angle on the second arm of the scattering stand, served to check the measurement of incident proton current.

The above equipment has proved to be very useful for studies of the angular dependence of nuclear reactions but suffers, at angles less than about 10°, from the limitation of requiring a very long external path for the protons if one is to avoid having the crystal detect protons scattered from the edges of the last antiscattering aperture of the input collimating system. For this reason we repeated our measurements at angles less than 20° with a gas scattering chamber designed specifically to investigate proton-proton scattering at angles down to 4°. A detailed description of this equipment will be published later by L. H. Johnston and D. A. Swenson.

The scattered protons incident on the NaI(Tl) detector gave rise to signals which were amplified by conventional electronic equipment and recorded on a ten-channel pulse-height analyzer. The previous studies of Eisberg[13] have served to prove that no significant number of inelastically scattered protons or disintegration products would be detected under the conditions of this experiment. Typical numbers *vs* pulse-height observations at $\theta_{c.m.}=10.4°$ and $\theta_{c.m.}=12.5°$ are shown in Fig. 2. Background effects with He removed from the scattering chamber were completely negligible at all angles of observation.

DISCUSSION AND EXPERIMENTAL DATA

To determine the yield of protons elastically scattered from helium at each angle, a pulse height-yield curve (Fig. 2) as obtained from the 10-channel energy discriminator was plotted. The first energy channel at

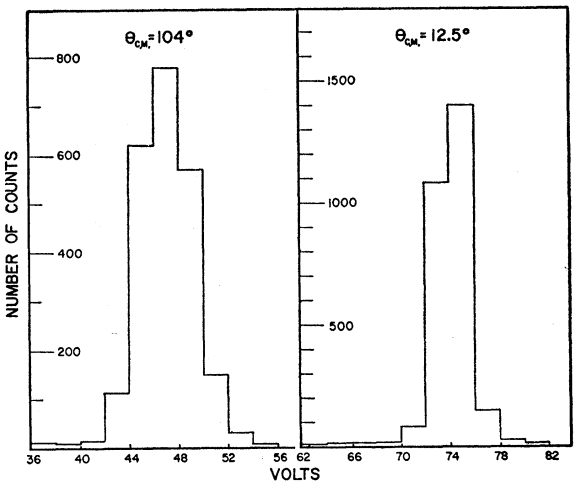

FIG. 2. Yield *vs* pulse-height histograms of the raw data. Volts refer to size of input signals into a 10-channel energy discriminator. At left is histogram of data taken at $\theta_{c.m.}=10.4°$, near minimum in $\sigma(\theta_{c.m.})$ shown in Fig. 3. Right hand figure is typical of low-angle data.

[13] R. Eisberg, Phys. Rev. **102**, 1104 (1955).

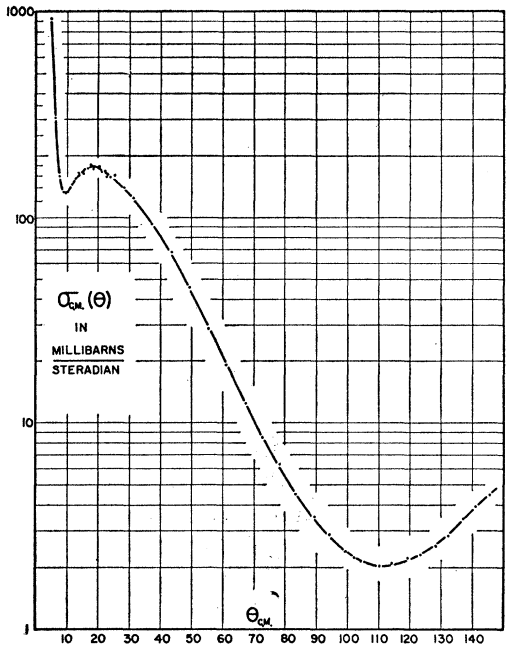

FIG. 3. Differential elastic scattering angular distribution of 39.8-Mev protons in He^4.

which the number of counts exceeded the background counts, together with all higher energy channels, were counted as elastically scattered protons from the helium. The background level contiguous to the elastic peak in all cases was less than 1% of the elastic counts recorded. The energy resolution (full width at half-maximum of the yield *vs* pulse-height curve) was approximately 6% for most data taking runs.

The formula used for calculating the cross sections was

$$\sigma_L(\theta_L)=\frac{kT}{P}\cdot\frac{Y}{N}\cdot\frac{\sin\theta_L}{G},$$

where Y is the yield of elastically scattered particles at laboratory angle θ_L, k is Boltzmann's constant, N the number of particles incident upon the target, P the helium gas pressure, T its temperature, and G a geometrical factor equal to Ad/Rl, where A is the area of the detector aperture, d the width of the volume defining collimation slit associated with the detector system, R the distance from the detector aperture to the center of the scattering chamber, and l the distance between the collimation slit and the detector aperture of the detector system. Through the course of the experiment, l was kept fixed. Four different values of the ratio Ad/R were utilized, however, to change the intensity of scattered particles and to vary the angular definition of the detector.

In the angular range 50° to 135° the angular definition of the scattered protons was ±4.75°, in the range 30° to 60° the angular definition was ±1.9°; the range 7.5° to 30° had angular definition ±0.95°, and the range 4° to 20°, ±0.55°.

Graphs of the differential cross section $\sigma_{c.m.}(\theta_{c.m.})$ are given in Figs. 3 and 4 as a function of center-of-mass angles, $\theta_{c.m.}$. Figure 4 is an expanded version of Fig. 3 to illustrate the details and the dispersion of experimental points more clearly. The points in the data represent average values of data taken in different runs, a "run" being defined as a continuous period of time in which data is collected. The standard deviation of the points is less than 2% for all points. The results are summarized in Table I. In virtually all cases, the runs which were averaged together were in themselves consistent within the statistical error. For angles of observation greater than 30°, most points represent the results of a single run. The reproducibility of points was in general found to be excellent. No correction was made at small scattering angles in the cross section for the finite width of the detector slits. The sole correction applied to the raw data was a 1.9% correction[14] to account for the number of protons lost from the elastic peak owing to nuclear interactions in the NaI crystal.

The accuracy of the results is attested to by the internal consistency of the data under different operating and detection conditions. No normalization was needed in going from one detection condition to another. For the calculation of the absolute cross sections, there exist the errors due to imperfect current collection and detector geometry, as well as errors in the pressure, temperature, and purity of the helium used, and an

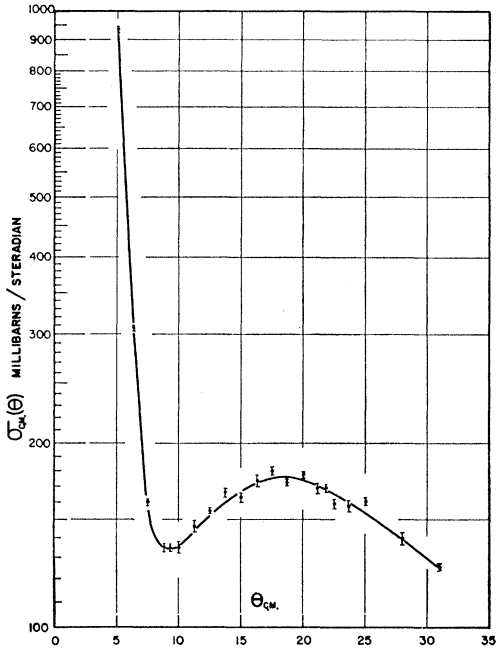

FIG. 4. Expanded version of Fig. 3 for the region of small scattering angles.

[14] Personal communication with L. H. Johnston and D. A. Swenson who determined the magnitude of this effect.

error due to the necessity of subtracting a finite background associated with the He scattered particles from the elastic peak of scattered protons. The errors are assigned as follows: beam current collection 1%, background 1%, geometry 2% (including effective widening of slits by the scattering of protons from the sides of the slits), pressure and temperature $\frac{1}{2}$% each, and the effect of impurities in the helium gas (important, if at all, at small scattering angles) of 1%. We can thus state that the absolute cross sections calculated are believed to be accurate to within $3\frac{1}{2}$%. The relative cross sections are, of course, somewhat better than this.

There are two general ways in which the data here presented could be analyzed; by a phase shift analysis as has been done at low energies, or by appeal to some kind of nuclear model to which the data is fitted, thereby providing one with a set of nuclear parameters, which employed with the particular model used, allows the fit to be made. Insofar as, for these relatively high proton energies, a phase shift analysis becomes quite complicated and probably not unambiguous, it was suggested by Professor W. B. Cheston that an optical model potential be used to attempt to explain the features of the curve. With a potential of the type $(V_0+iW_0)\rho(r) = V(r)$, where $\rho(r)$ is a form factor, and V_0 and W_0 are numbers characteristic of the strengths of the real and imaginary parts of the potential well, attempts to fit the data are being undertaken at this laboratory. Because the alpha particle is a tightly bound structure, we have some confidence that a potential well produced by the collective effect of all the nucleons would describe well the scattering process. It might also be expected, however, from the known spin orbit effects of low-energy elastic scattering that a simple V_0+iW_0 might not suffice to give a satisfactory description.

TABLE I. Observed differential cross sections in millibarns per steradian for elastic scattering of 39.8-Mev protons from He^4. Cross sections are in the center-of-mass system. The standard deviation for each angle is also given.

$\theta_{c.m.}$	$\sigma_{c.m.}$	S.D. in %	$\theta_{c.m.}$	$\sigma_{c.m.}$	S.D. in %	$\theta_{c.m.}$	$\sigma_{c.m.}$	S.D in %
5.08	910	±1.6	21.20	164.1	±1.9	78.2	6.14	±1.8
6.26	300.2	1.03	21.85	165.2	1.4	83.4	4.44	1.4
7.51	156.5	1.5	22.47	155.0	1.4	89.0	3.41	1.9
8.77	131.5	1.75	23.72	153.9	2.0	94.0	2.81	2.0
9.38	131.5	1.5	24.93	156.9	1.45	99.4	2.30	1.9
10.02	131.5	1.9	28.0	136.5	1.9	104.4	2.09	2.1
11.25	143.5	1.9	31.1	122.8	1.4	109.6	1.977	2.0
12.50	151.4	0.96	37.2	91.80	0.40	114.4	1.885	2.0
13.75	162.0	1.6	43.3	67.6	1.8	119.2	2.16	1.9
15.03	159.1	1.7	49.4	44.8	2.0	123.4	2.27	1.9
16.32	169.2	2.0	55.4	28.4	2.0	128.0	2.51	2.0
17.50	175.7	1.3	61.2	18.88	1.1	132.4	2.80	1.9
18.73	169.1	1.0	67.0	12.45	1.35	136.6	3.38	2.0
19.98	173.2	1.8	72.6	8.33	1.3	140.8	3.87	1.8
						146.0	4.62	1.9

The present results resembles data taken at Harvard[12] where the forward minimum was first observed. Though two principal minima occur in $\sigma(\theta)$ in both experiments, no indication was found here of any other inflections as was found at $\theta_{c.m.}=60°$ in the Harvard data.

ACKNOWLEDGMENTS

We would like to acknowledge our indebtedness to Professor W. B. Cheston and Professor A. E. Glassgold for their suggestions and interest in this experiment, and to Professor L. H. Johnston and Mr. D. A. Swenson for the use of their proton-scattering apparatus. To these and to the whole operating crew of the linear accelerator we express our gratitude.